Electronic Supplementary Material (ESI) for Dalton Transactions.
This journal is © The Royal Society of Chemistry 2022

Electronic Supplementary Information

Parahydrogen-induced polarization study of imine hydrogenations mediated by a metal-free catalyst

Danila O. Zakharov,[a] Konstantin Chernichenko,[b,c] Kristina Sorochkina,[a,b] Timo Repo[b] and Vladimir V. Zhivonitko*[a]

[a.] NMR Research Unit, Faculty of Science, University of Oulu, P.O. Box 3000, Oulu, 90014, Finland. E-mail: vladimir.zhivonitko@oulu.fi
[b.] Department of Chemistry, University of Helsinki, A. I. Virtasen Aukio 1, 00014 Helsinki, Finland
[c.] Present address: Discovery, Product Development & Supply (DPDS), Janssen Pharmaceutical Companies of Johnson & Johnson, Turnhoutseweg 30, 2340 Beerse, Belgium

Contents

1 General information

1.1 Instruments and chemicals

Multinuclear NMR spectra were acquired on a 400 MHz Bruker AV 400 NMR spectrometer equipped with a broad-band 5 mm radiofrequency probe. Parahydrogen-enriched H_2 gas (92%) referred to in the main text as simply para-H_2 was produced using a Bruker parahydrogen generator. Certain control experiments described in the main manuscript were performed at a higher magnetic field on a 600 MHz Bruker AV 600 NMR spectrometer.

QCAT catalyst, 1-{2-[Bis(pentafluorophenyl)boryl]benzyl}-2,2,4,7-tetramethyl-1,2,3,4-tetrahydroquinoline, was prepared from 2-bromobenzyl bromide by previously known synthetic technique.[S1] For the presented experiments, we used the catalyst that was isolated and purified by recrystallization in QCAT-H_2 form. Imines 1a-4a were prepared according to reported the procedures.[S2] Amines 1b-4b are all known compounds and their ^{1}H and ^{13}C NMR data matched the literature data. Amines used in the control experiments (1b and 1,2,3,4-tetrahydro-2,2,4,7-tetramethylquinoline (5b)) were purchased from Merck.

1.2 Para-H_2 experiments

NMR samples were prepared by preparing solutions of QCAT (0.04 mmol) in 0.420 mL of dry degassed toluene-d8 in 5 mm Wilmad gas-tight NMR tubes (medium wall) and adding 0.13 mmol of desired imines (1a-4a) under inert atmosphere. Experiments were performed at temperatures ranging from 330 to 360 K; the temperatures are indicated in each experiment described below.

In the first type of experiments, the sample tubes were charged with 6 bar of para-H_2, avoiding gas-liquid mixing. Thereafter, tubes were vigorously shaken for ca. 2-3 s just before insertion to the NMR magnet, placed inside spectrometer, and NMR spectra were recorded. A single shake of the tube allowed measuring several ^{1}H NMR spectra before para-H_2 was completely converted into normal H_2 and the hyperpolarization completely decayed, or before the completion of the reaction. In the second approach, para-H_2 was bubbled through the reaction solution under the para-H_2 overpressure for 10 s, and then the parahydrogen flow was abruptly switched off and a ^{1}H NMR spectrum was recorded.

The observed hyperpolarization effects in ^{1}H NMR spectra measured with $\pi/4$-pulses typically revealed antiphase character of B-H group resonances for QCAT-H_2 molecule, which was practically independent whether the measurement performed immediately after the insertion of after some time the samples spent in the magnet. This indicated that in all cases we observed PASADENA type hyperpolarization,[S3,S4] i.e., predominantly the hyperpolarization of species that were generated inside the NMR magnet.

2 Hyperpolarization of amine products

In this section, we present a larger scheme of the catalytic cycle of imine hydrogenation using QCAT and para-H_2 (Scheme S1), a description of the method used to determine enhancement factors, and NMR spectra supporting the discussions in the main text.

2.1 Mechanism of imine hydrogenation over QCAT

The mechanism of imine hydrogenation over QCAT includes four stages (Scheme S1), as was proposed by Sumerin et al.[S1] Firstly, hydrogen molecule is activated by QCAT, yielding QCAT-H_2 adduct (Step I). After that a proton transfer from NH group of QCAT-H_2 to imine nitrogen atom occurs which results in the formation of an unstable ionic pair intermediate (Step II). Secondly, the final proton transfer from activated catalyst leads to QCAT-amine adduct, connected via a dative bond (Step III). The last step of hydrogenation cycle releases the amine product and recovers the catalyst (Step IV). The present study indicates the reversibility of all these steps.

Scheme S1. Mechanism of imine hydrogenation over QCAT catalyst.

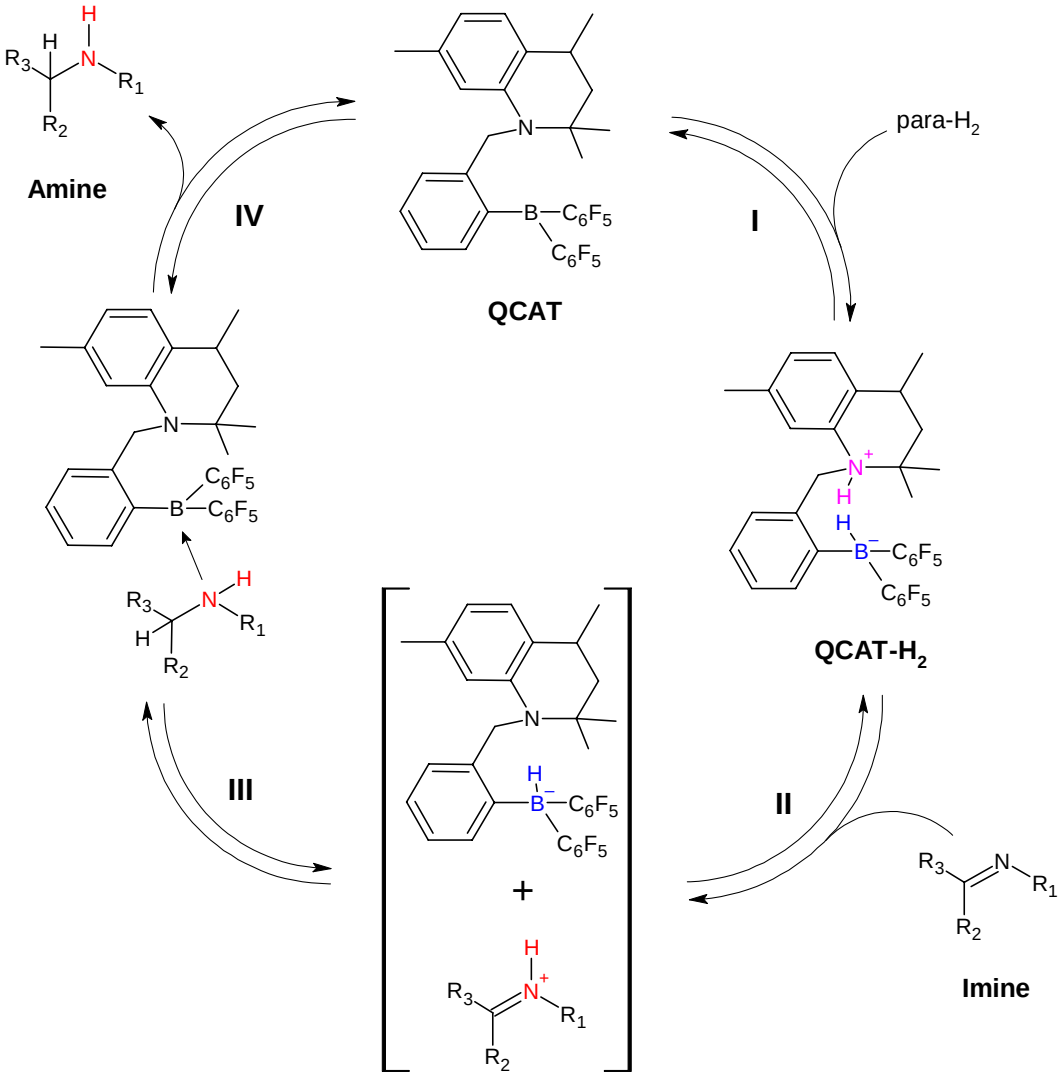

In the presence of para-H_2, ^1H hyperpolarization of QCAT-H_2 molecule is generated (see Figures S1-S5, the corresponding areas are marked with purple circles for N-H protons and with blue circles for B-H in the spectra shown below; see also discussion the in the main text). This is consistent with the Step I of the catalytic cycle. We observed a substantial negative net polarization of N-H groups in amine products using ^1H NMR measurements, see signals marked with doted rectangles and red "N-H" label below. In accord with Step II of the catalytic cycle, this observation indicates a transfer of the hyperpolarized proton originating from para-H_2 molecule to the hydrogenation product via the QCAT-H_2 intermediate. In some cases, the reversibility of the hydrogen transfer at Step III to carbon atom of the double bond enabled the hyperpolarization of C-H groups hydrogens of amine products which are marked with doted rectangles and black "C-H" labels in the figures. Those signals typically overlap the signal of hyperpolarized B-H group proton of QCAT-H_2.

The hydrogenation at the elevated temperatures (340-360 K) typically led to a complete imine conversion into the corresponding amine product in 20-30 min since the beginning of the reaction.

Experiments at 360 K (see Figures S1 and S4) demonstrated higher signal enhancements for QCAT-H_2 and amine product protons as compared to those at 340 K. At 360 K, we also clearly observed negative net polarization of C-H group hydrogen in the amine product in addition to the N-H group negative net polarization observed also at lower temperatures (compare Figure S1a and Figure 1a in the main text).

2.2 ^{1}H NMR signal enhancements for amine products

^{1}H NMR signal enhancement factors were estimated by comparing absolute integral amplitudes of enhanced and thermal N-H group signals of corresponding amines produced within ca. 20 s time frame by acquiring single scan spectra, see Table S1.

Table S1. ^{1}H NMR signal enhancements of amine product 1b-4b.

Amine (N-H proton)	Enhancement factor[a]	Chemical shift, ppm
1b	10	3.40
2b	15	3.45
3b	7	3.47
4b	10	3.32

[a]As measured at 340 K

The procedure provided a lower limit of the enhancement since the product accumulation time was not optimized with respect to the nuclear spin relaxation rate. In principle, optimization of the time frame could allow an optimal scan accumulation of the hyperpolarized signal, as para-H_2 was present in the solution for a relatively long time and the hyperpolarization was produced continuously. A precise measurement of the enhancement factors and optimization of reaction conditions are out of the scope of this initial study. Nevertheless, the currently provided enhancement factors characterize the potential of QCAT: at least an order of magnitude signal enhancements are observable.

2.3 Experimental spectra

2.3.1 Hydrogenation of N-(4-methylphenyl)-1-phenylethan-1-imine (**1a**) with para-H_2

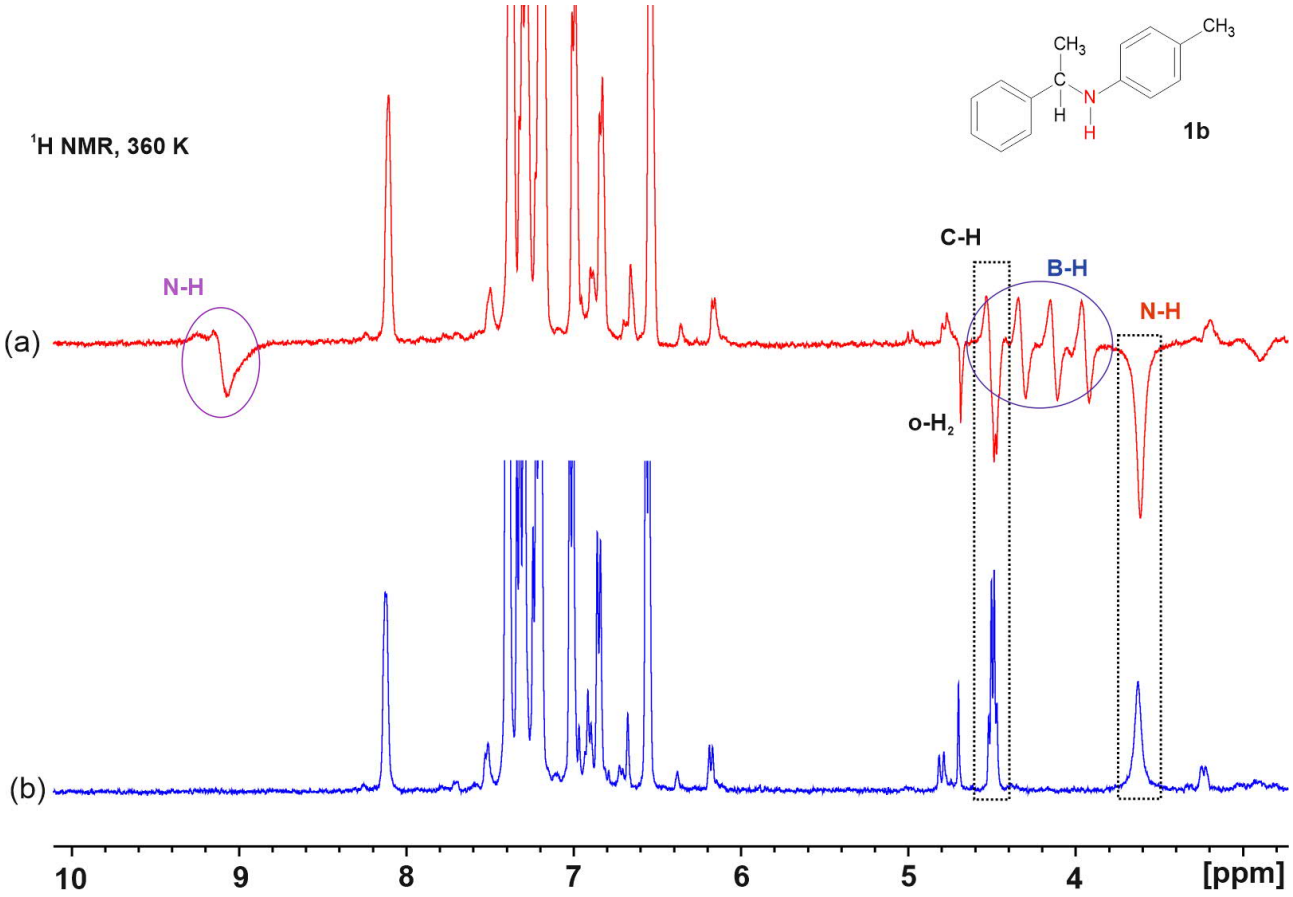

Figure S1. ^{1}H NMR spectra acquired in hydrogenation of imine 1a with para-H_2 using QCAT at 360 K. For this experiment, we bubbled para-H_2 through the solution of the same concentrations of reagents and the catalyst as in the experiment at 340 K (Figure 1 in the main text). Spectrum (a) with the hyperpolarization demonstrate enhanced proton resonances for N-H/B-H groups in QCAT-H_2 (ovals) and N-H/C-H (rectangles) groups in amine product 1b. The enhanced in-phase negative signal of C-H group hydrogen was detected, which wasn't visible in experiments at lower temperatures. Spectrum (b) was recorded 1 minute after para-H_2 bubbling when the spins relaxed to thermal equilibrium.

2.3.2 Hydrogenation of N-(3,5-dimethylphenyl)-1-phenylethan-1-imine (**2a**) with para-H_2

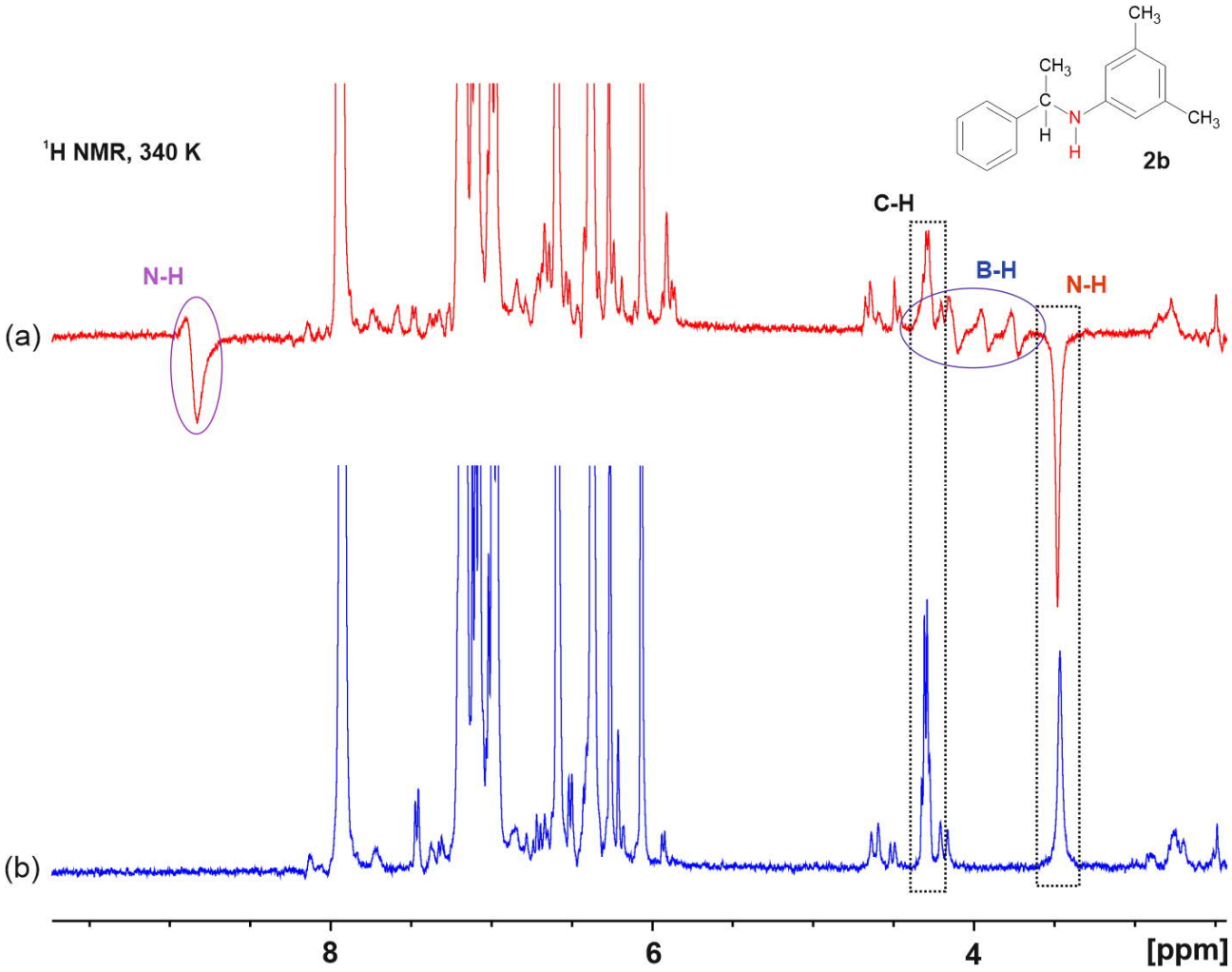

Figure S2. ^{1}H NMR spectra acquired in hydrogenation of imine 2a with para-H_2 using QCAT at 340 K. Red spectrum (a) was acquired at the beginning of the hydrogenation just after introducing para-H_2 into a reaction mixture. The enhanced signals corresponding to N-H and B-H group hydrogens of QCAT-H_2 adduct are shown with ovals. The enhanced in-phase signal corresponds to N-H group hydrogen of amine product 2b. C-H group hydrogen of 2b originating also from para-H_2 feedstock showed thermal polarization. The signals of 2b are shown with rectangles. Blue spectrum (b) was recorded 5 minutes after addition of para-H_2 after relaxation of the hyperpolarization.

2.3.3 Hydrogenation of N-(3-methylphenyl)-1-phenylethan-1-imine (**3a**)

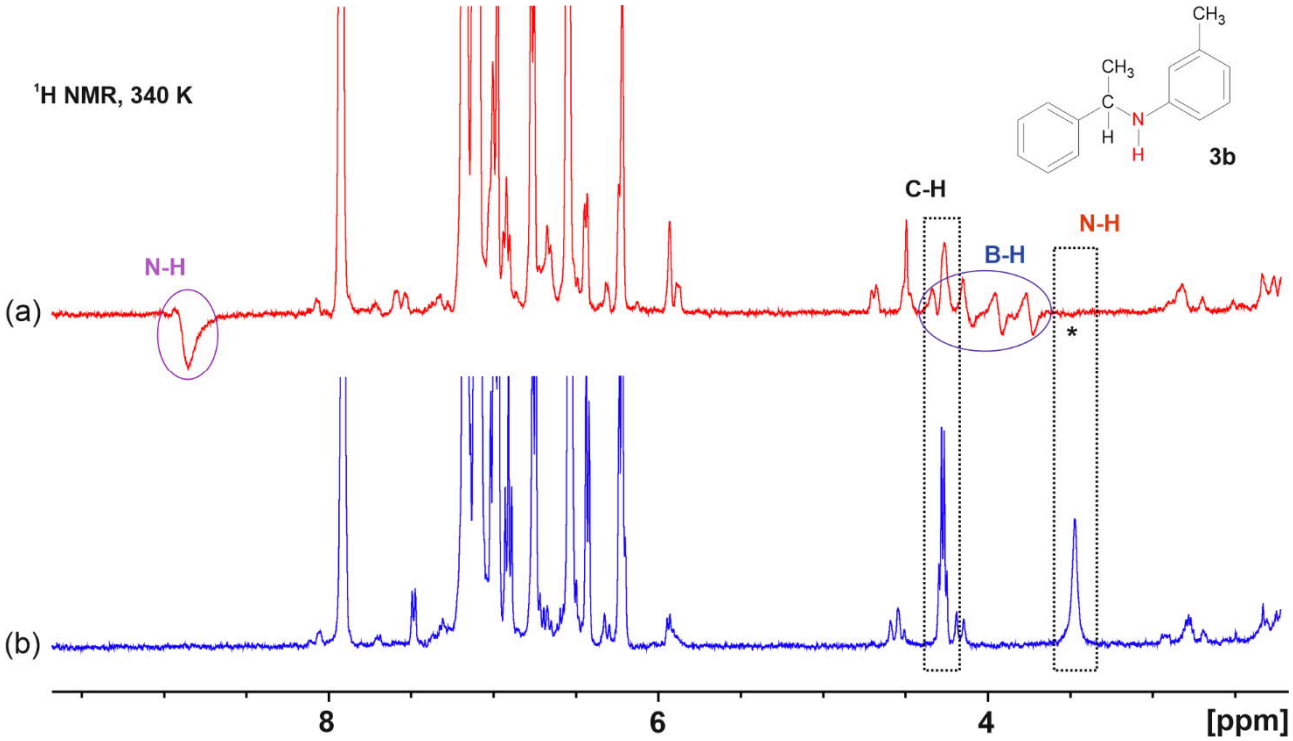

Figure S3. ^{1}H NMR spectra acquired in hydrogenation of imine 3a with para-H_2 using QCAT at 340 K. Red spectrum (a) was acquired at the beginning of hydrogenation just after introducing para-H_2 into a reaction mixture. The enhanced signals corresponding to N-H and B-H group hydrogens of QCAT-H_2 adduct are shown with ovals. The signal of N-H group hydrogen of 3b is disappeared after introducing para-H_2; its position is marked with an asterisk. C-H group hydrogen of 3b originating also from para-H_2 feedstock showed thermal polarization. The signals of 3b are shown with rectangles. Blue spectra (b) was recorded 1 min after addition of para-H_2 after relaxation of the hyperpolarization.

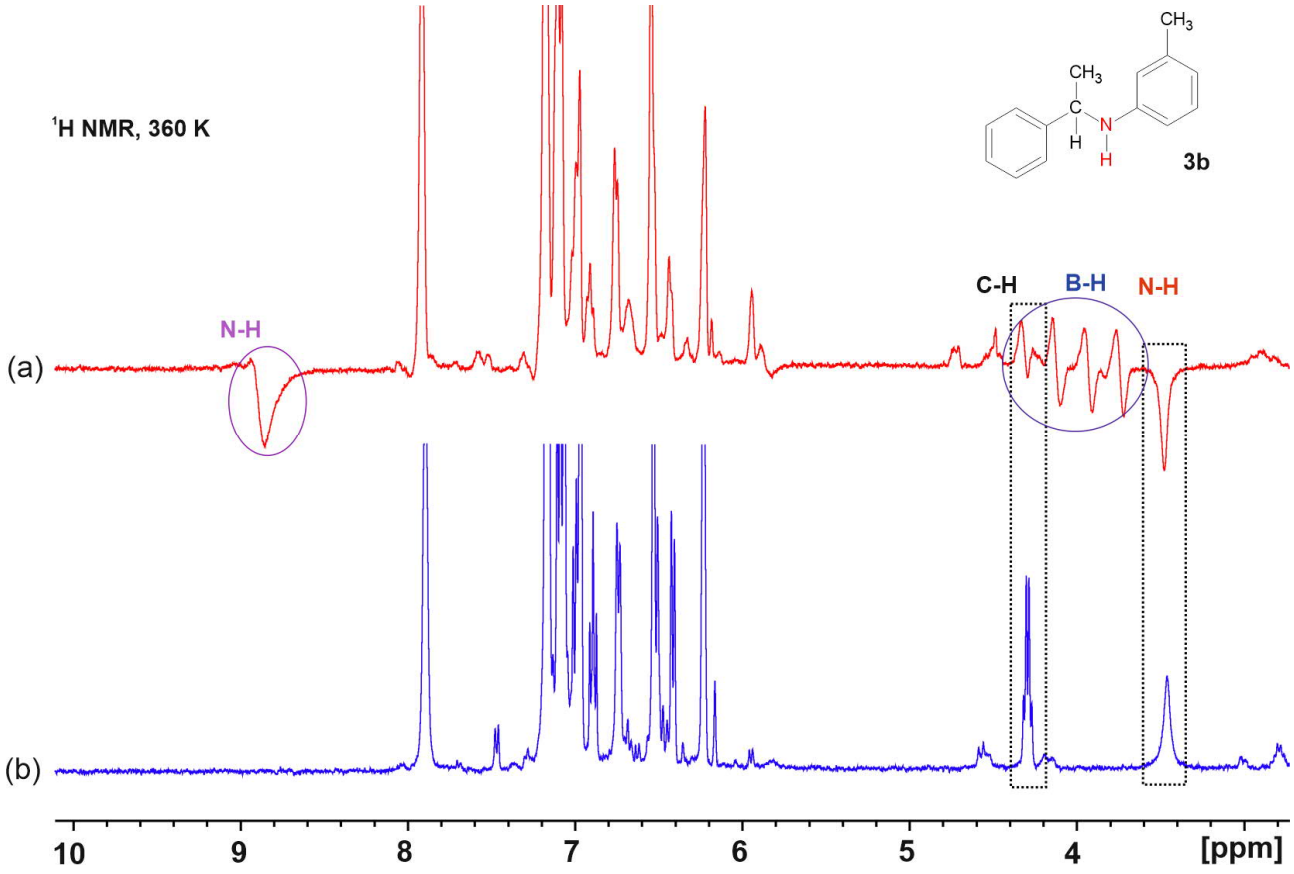

Figure S4. ^{1}H NMR spectra acquired in hydrogenation of imine 3a with para-H_2 using QCAT at 360 K. The same concentrations of the imine and the catalyst as in the experiment at 340 K (Figure S3) were used. Hyperpolarization spectrum (a) demonstrated stronger enhanced signals both for QCAT-H_2 (N-H/B-H groups) and the amine product 3b (N-H group) at 360 K as compared to 340 K. The signal of C-H group hydrogen of 3b disappeared, indicating a slight hyperpolarization of the corresponding proton. Ovals and rectangles are used to show signals of QCAT-H_2 and amine product 3b, respectively. Spectrum (b) was recorded 3 minutes after adding para-H_2 to the solution when the spins relaxed to thermal equilibrium.

2.3.4 Hydrogenation of N-(4-methoxyphenyl)-1-phenylethan-1-imine (**4a**)

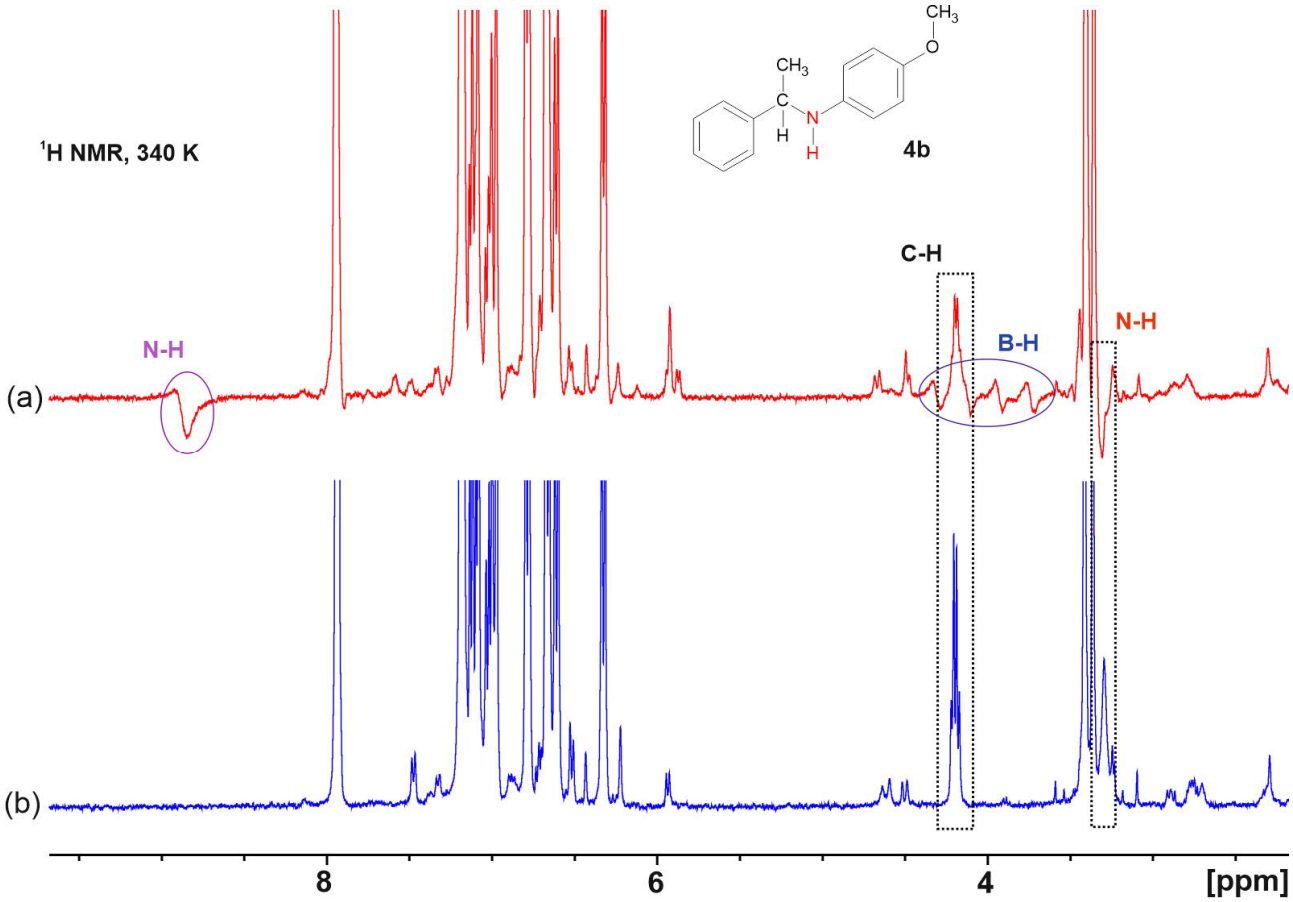

Figure S5. ^{1}H NMR spectra acquired in hydrogenation of imine 4a with para-H_2 using QCAT at 340 K. Red spectrum (a) was acquired at the beginning of hydrogenation just after introducing para-H_2 into a reaction mixture. The enhanced signals corresponding to N-H and B-H group hydrogens of QCAT-H_2 adduct are shown with ovals. The enhanced in-phase signal corresponds to N-H group hydrogen of amine product 4b. C-H group hydrogen of 4b originating also from para-H_2 feedstock showed thermal polarization. The signals of 4b are shown with rectangles. Blue spectrum (b) was recorded 2 min after addition of para-H_2 after relaxation of hyperpolarization.

2.4 Comparison of hyperpolarization effects in different magnetic fields

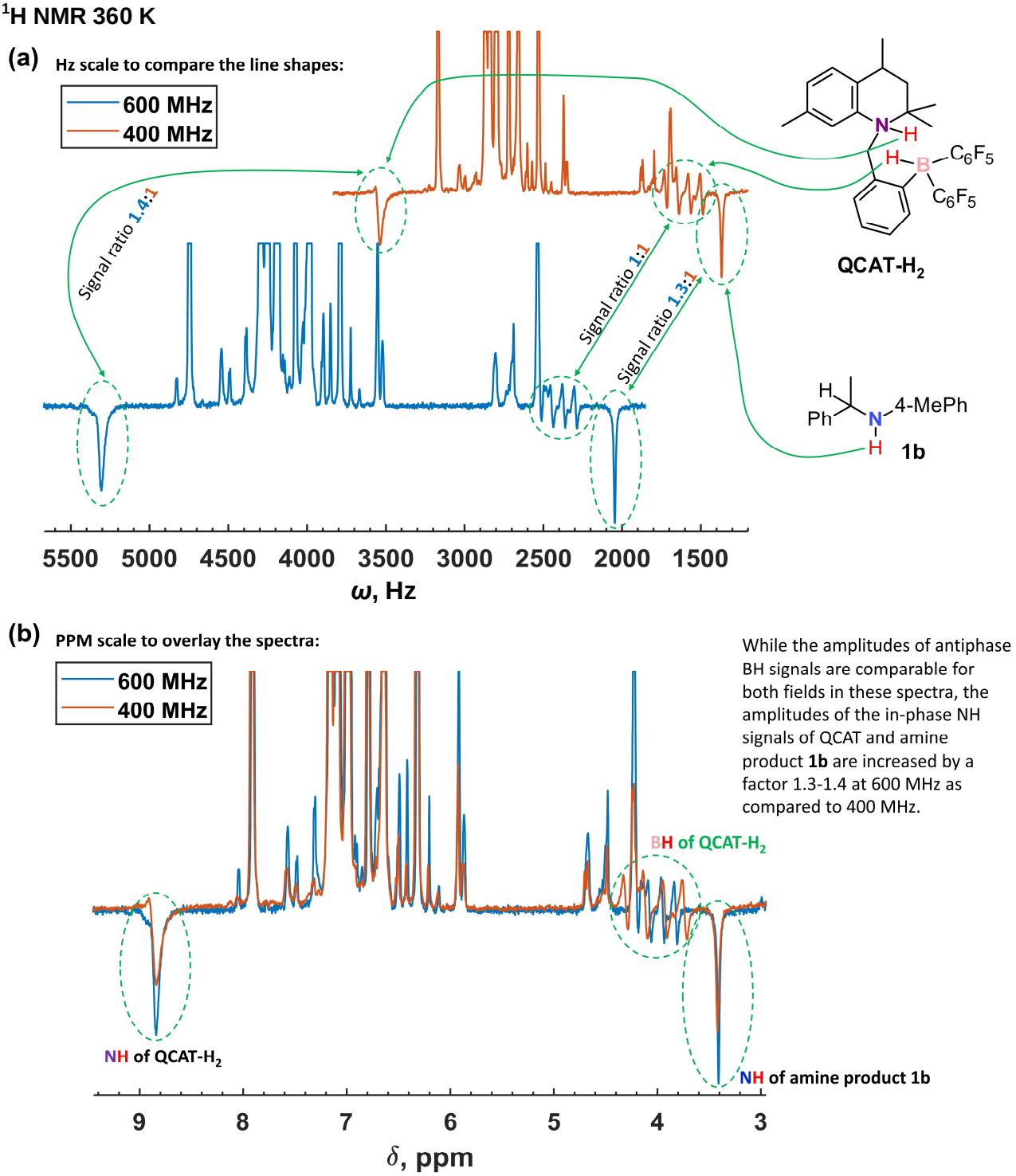

Figure S6. Comparison of ^{1}H NMR hyperpolarization effects observed in hydrogenation of imine 1a with para-H_2 over QCAT catalyst at 9.4 and 14.1 T. (a) The spectra shown using frequency scale in Hz to have the natural comparison of line widths. The negative net polarization signals of NH groups of QCAT-H_2 and product 1b are stronger by a factor of 1.3-1.4 in the case of 14.1 T (600 MHz) as compared to 9.4 T (400 MHz). The increase of the amplitude with the magnetic field strength indicates that chemical shift anisotropy indeed can play a crucial role for the creation of the single-spin negative net polarization from the parahydrogen spin order. (b) The same spectra shown using ppm scale for comparison of peak positions in the spectra at the different magnetic fields. The same concentrations of the reagents are used as in the experiment in Fig. 1 (main text).

3 Hyperpolarization of N-(4-Methyl)phenyl-1-phenylethylideneamine (1b) and 1,2,3,4-tetrahydro-2,2,4,7-tetramethylquinoline (5b) over QCAT without formal hydrogenation

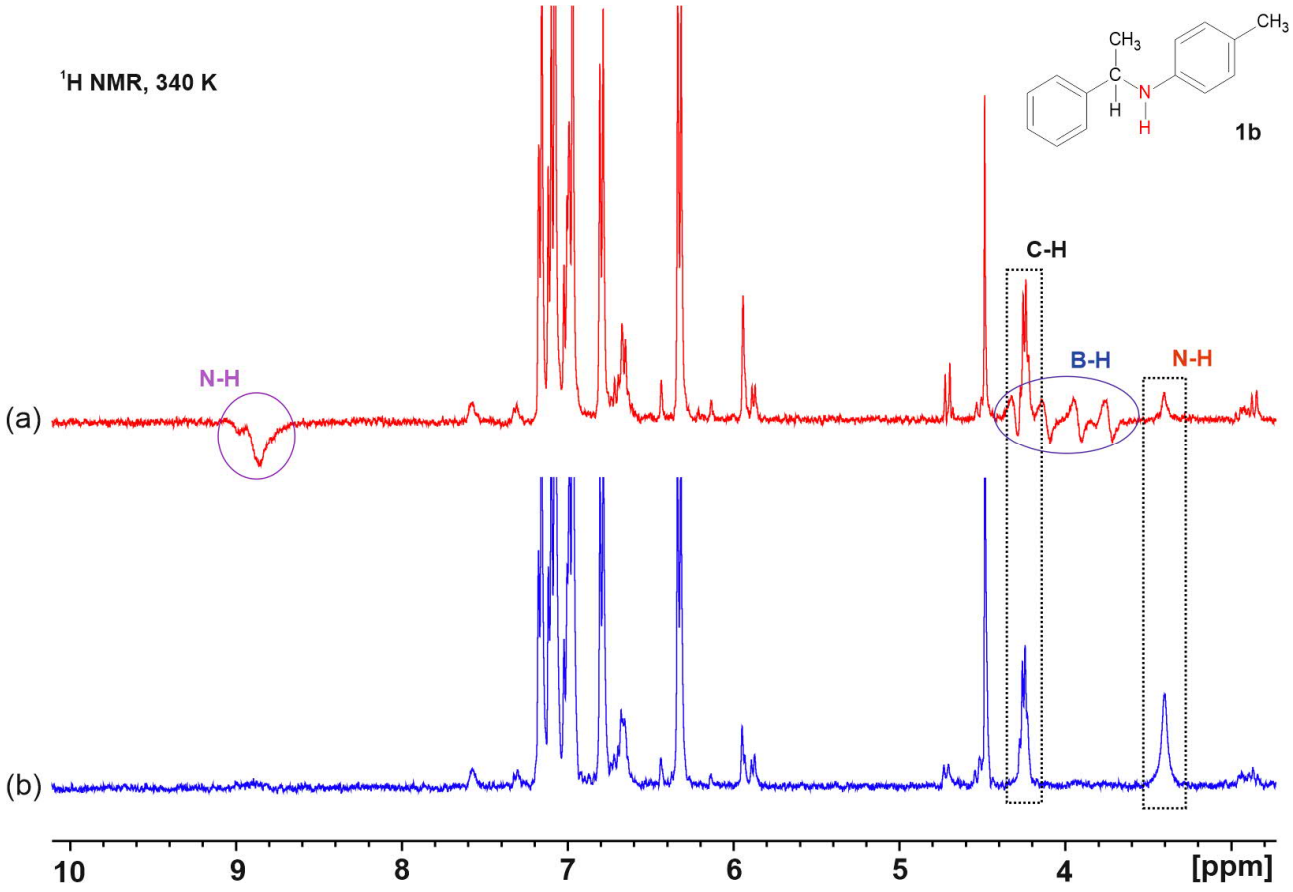

Figure S7. ^{1}H NMR spectra acquired in reaction of amine 1b (0.04 mmol) with QCAT (0.04 mmol) under para-H_2 atmosphere at 340 K. Spectrum (a) was acquired after introducing para-H_2 into the solution. The enhanced signals corresponding to N-H and B-H group hydrogens of QCAT-H_2 adduct are shown with ovals. The signal of amine N-H proton has much lower amplitude as compared to the thermal spectrum (b), showing a weak hyperpolarization effect. The signals of 1b and QCAT-H_2 are shown with rectangles and ovals, respectively. The thermal spectrum (b) was recorded 6 min after shaking the tube with para-H_2.

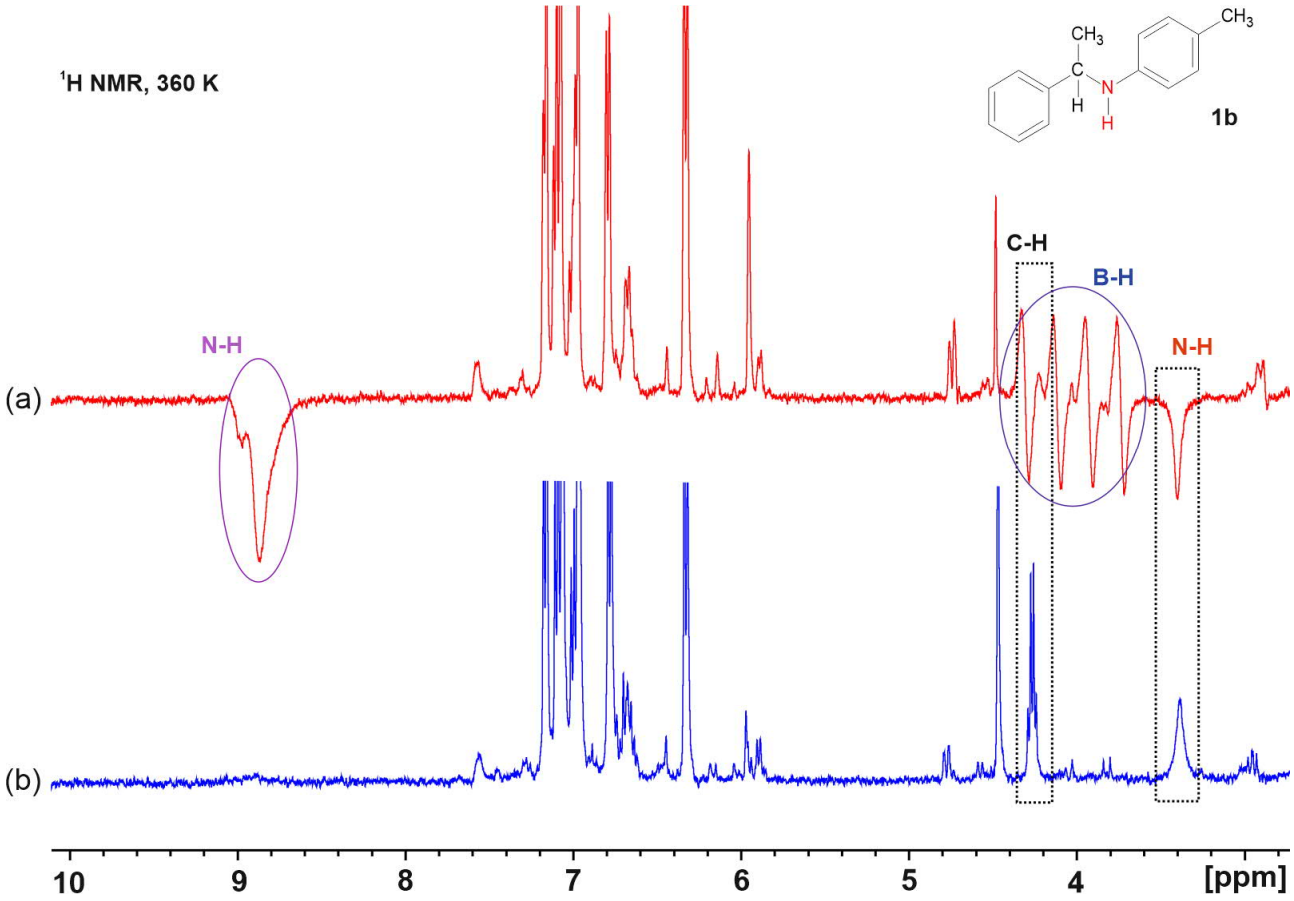

Figure S8. ^{1}H NMR spectra acquired in reaction of amine 1b with QCAT under para-H_2 atmosphere at 360 K. The same sample as in the experiment at 340 K (Figure S7) was used. Spectrum (a) was recorded after shaking the tube charged with fresh portion of para-H_2. Both N-H and C-H group signals of 1b showed negative net hyperpolarization that was stronger than that in the corresponding experiment at 340 K. The signal of N-H amine proton demonstrates negative signal. The C-H signal of amine is vanished which indicated the presence of a weak negative hyperpolarization of that hydrogen. The signals of 1b and QCAT-H_2 are shown with rectangles and ovals, respectively. Spectrum (b) was recorded after relaxation of the hyperpolarization (5 min later).

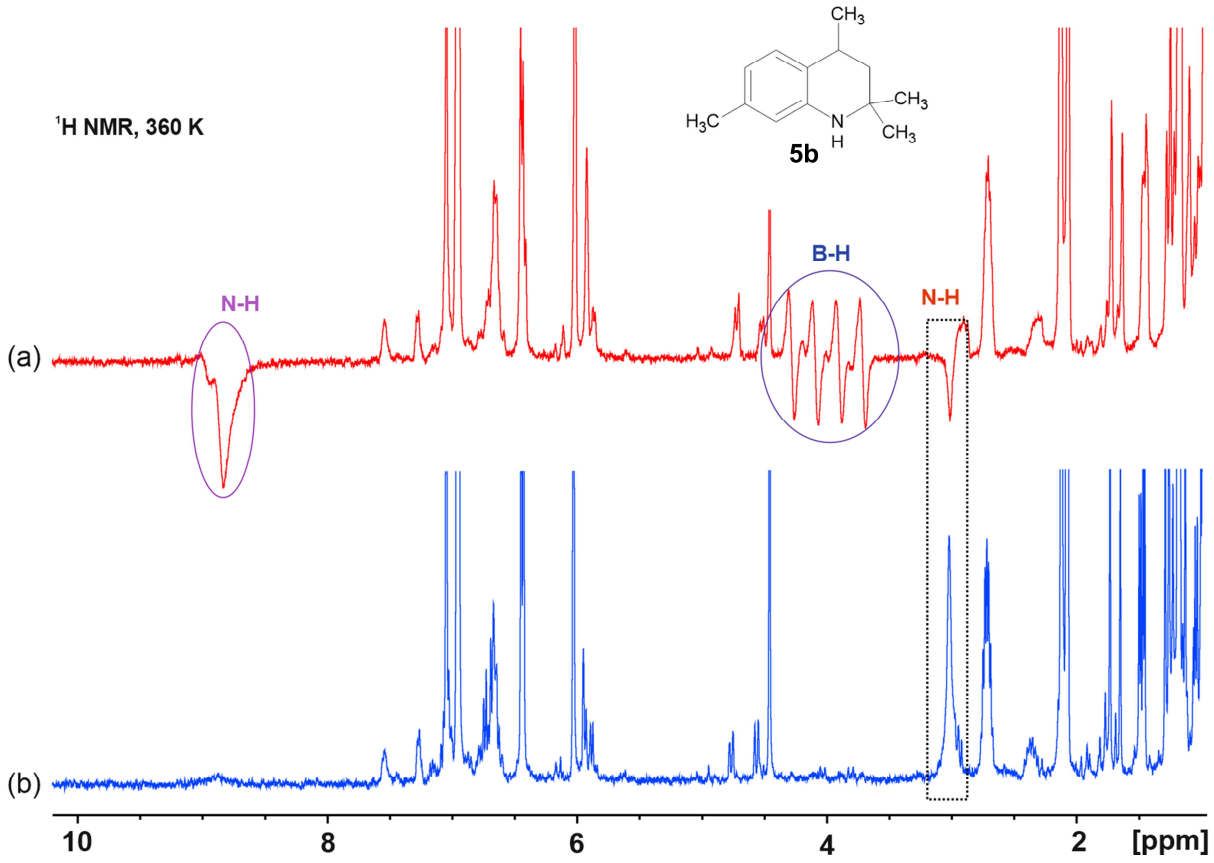

Figure S9. ^{1}H NMR spectra acquired in the reaction of 1,2,3,4-tetrahydro-2,2,4,7-tetramethylquinoline (5b) with QCAT under para-H_2 atmosphere at 360 K. No hyperpolarization was observed at 340 K for the amine. Spectrum (a) was recorded after shaking the tube charged with fresh portion of para-H_2. The N-H group signal of 1,2,3,4-tetrahydro-2,2,4,7-tetramethylquinoline (5b) revealed the negative net polarization; the signal of N-H proton of the amine demonstrates negative signal. The N-H signals of 1,2,3,4-tetrahydro-2,2,4,7-tetramethylquinoline (5b) and QCAT-H_2 are shown with rectangles and ovals, respectively. Spectrum (b) was recorded after relaxation of the hyperpolarization (5 min later).

4 Experiments with lower loading of QCAT

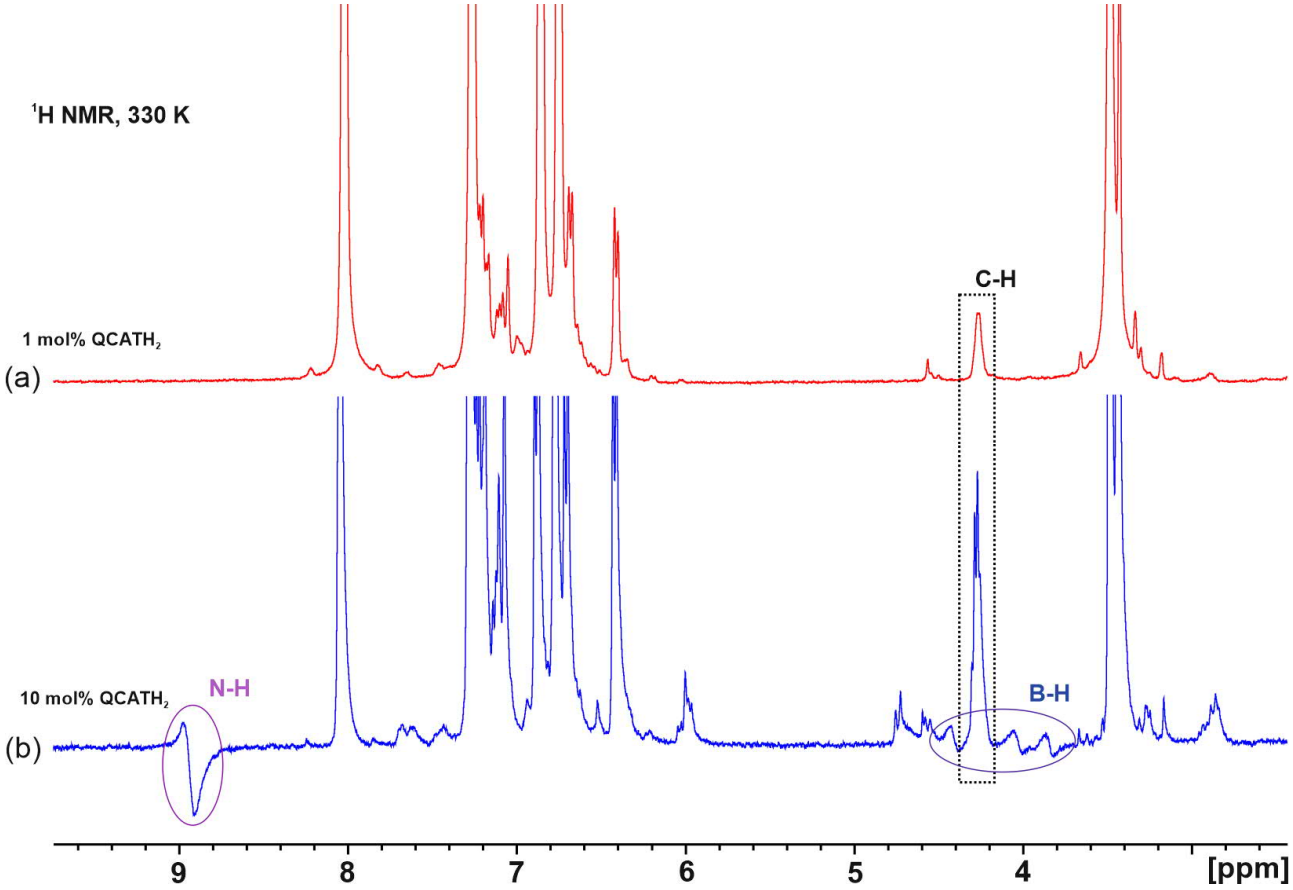

Figure S10. Spectrum (a) was recorded immediately after introducing para-H_2 into a mixture of 1.05 mmol of imine 4a and 1 mol% of QCAT. The enhanced signals were not observed, in spite of the fact that there was a slow accumulation of product 4b. Spectrum (b) was recorded after introducing para-H_2 to a solution of 10 mol% of QCAT and 0.35 mmol of imine 4a. Enhanced signals of N-H and B-H group hydrogens of QCAT-H_2 were observed (see ovals). Although we observed accumulation of amine product 4b, we couldn't detect any clear sign of hyperpolarization of that molecule. The signal of N-H proton of 4b is difficult to see because of it is overlapped by the signal from OCH_3 protons at 3.4 ppm. Both spectra were acquired at 330 K. The C-H signal of 4b is shown with a rectangle.

5 Intermolecular FLPs

5.1 Hydrogenation of imines using boranes as Lewis acid catalysts

Scheme S2. Hydrogenation of imine 2a using boranes as Lewis acids.

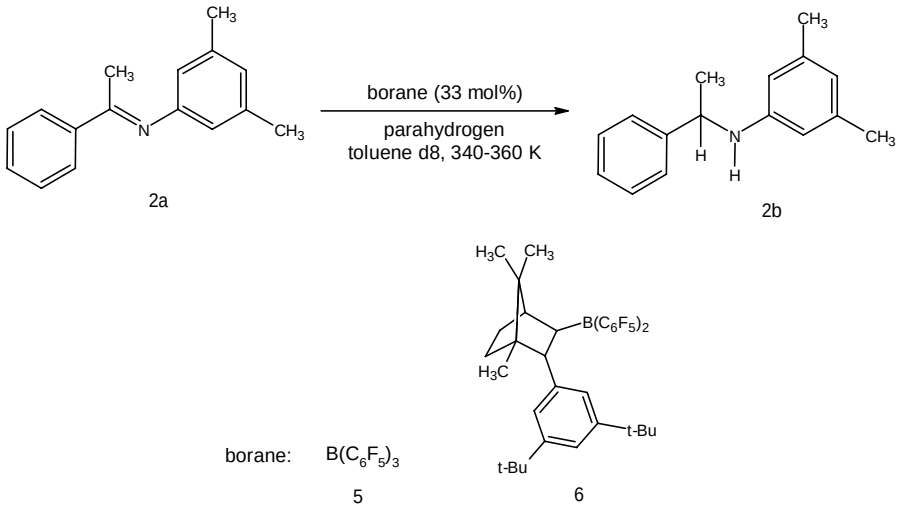

Scheme S3. Catalytic cycle for imine reduction involving H_2 activation by imine/borane pair.

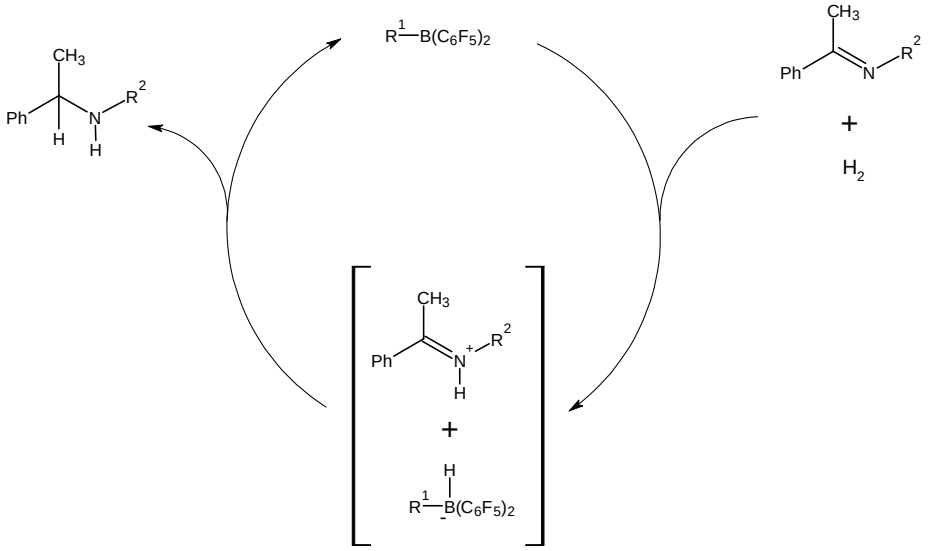

In the literature, it was described that imines could be hydrogenated using various $B(C_6F_5)_3$ derivatives as Lewis acid catalysts.[S5,S6] Basically, in that cases borane acts as Lewis acid, while imine substrate acts as a Lewis base. Hydrogen molecule is split by the resulting FLP, giving two intermediates that consequently undergo hydride transfer from borate to imine to yield the amine product (Scheme S3). Herein, we tested hydrogenations of imine 2a with para-H_2 using boranes 5 and 6 (se Scheme S2) as Lewis acids.

5.1.1 Hydrogenation of **2a** using $B(C_6F_5)_3$ (**5**)

In this experiment, we used a solution of 0.14 mmol of 2a and 0.047 mmol (33 mol%) of $B(C_6F_5)_3$ (borane 5, Scheme S2) in toluene d8. Para-H_2 was introduced into the mixture by shaking the sample tube charged with 6 bar of para-H_2.

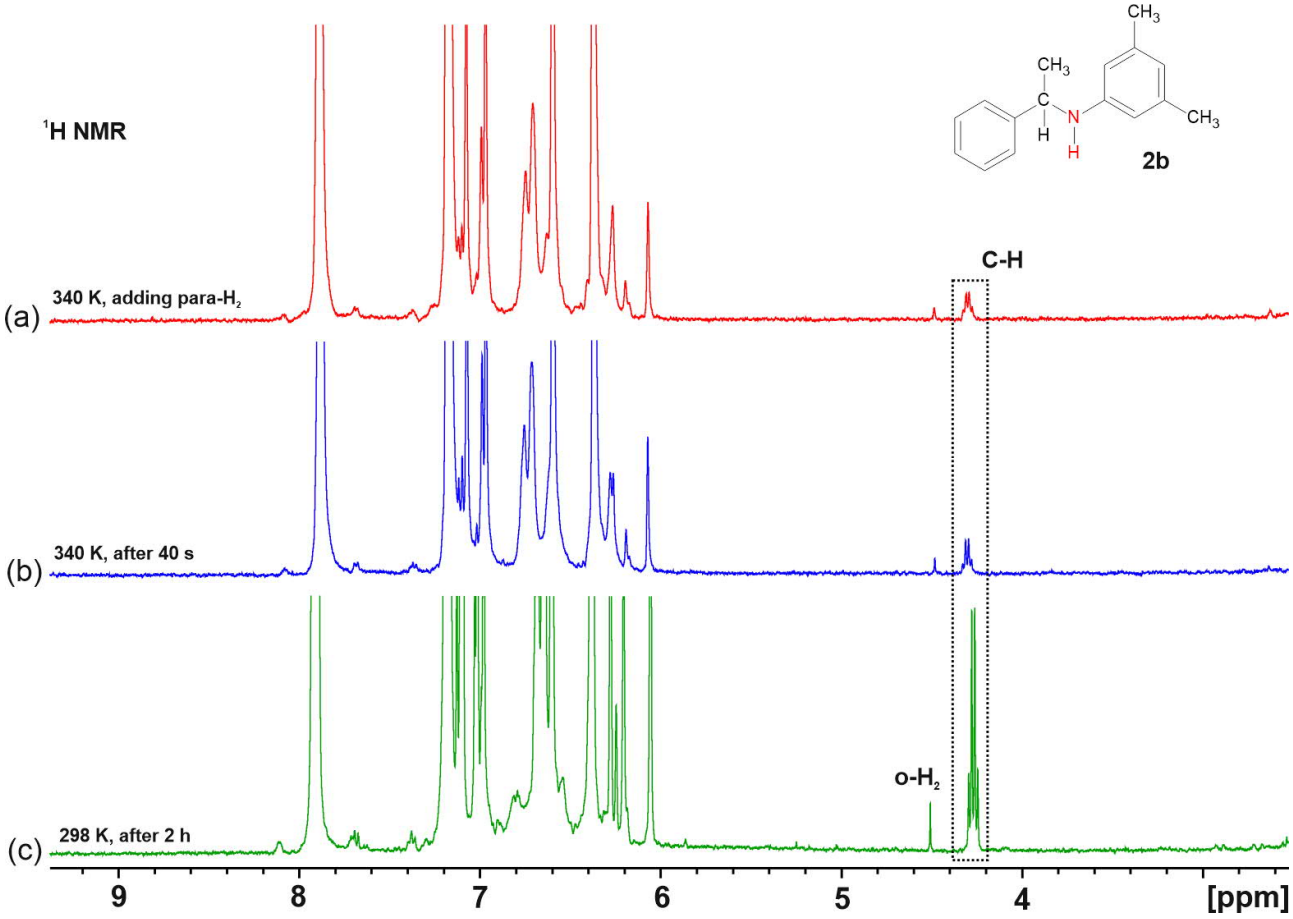

Figure S11. ^{1}H NMR spectra acquired in hydrogenation of imine 2a with para-H_2 using $B(C_6F_5)_3$. Spectrum (a) was recorded at 340 K after shaking the sample tube with a fresh portion of para-H_2. Spectrum (b) was acquired 40 s later. We couldn't observe any enhanced signals, neither from NH/BH intermediates nor from the reaction product. Spectrum (c) recorded after cooling the solution to 298 K shows a significant accumulation of amine product 2b, meaning that the reaction was active under the used experimental conditions.

5.1.2 Hydrogenation of **2a** using ((1R,2R,3R,4S)-4,7,7-trimethyl-3-(3,5-di-tert-butylphenyl)lbicyclo[2.2.1]heptan-2-yl)bis(perfluorophenyl)-borane (**6**)

In the experiment with borane 6 (Scheme S2) we used a solution of 0.11 mmol of 2a and 0.036 mmol (33 mol%) of the borane in toluene-d8. Similarly as in the experiment with $B(C_6F_5)_3$, para-H_2 was introduced into the reaction mixture by shaking the sample tube charged with 6 bar of parahydrogen.

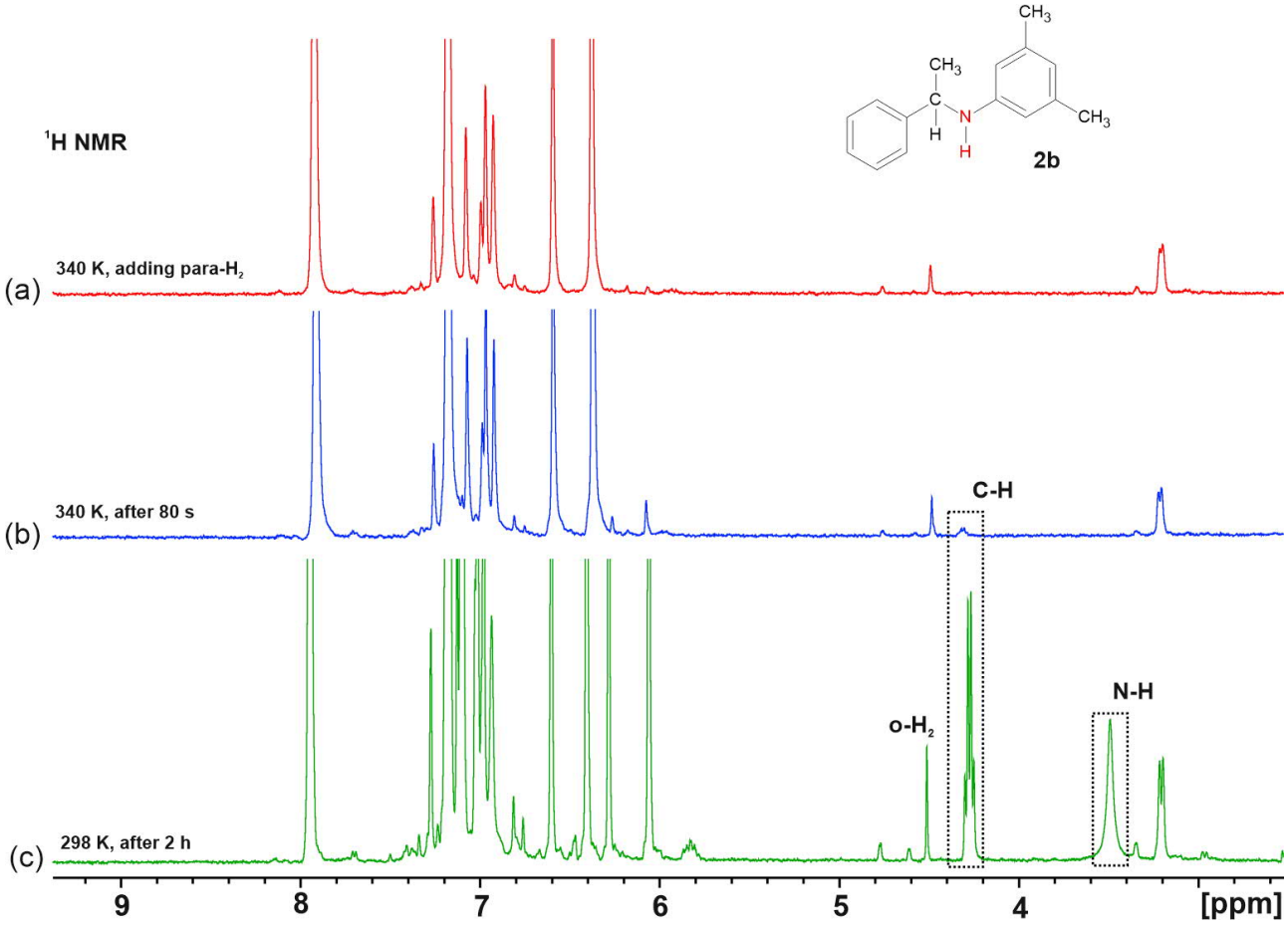

Figure S12. ^{1}H NMR spectra acquired in hydrogenation of imine 2a with para-H_2 using borane 6. Spectrum (a) was recorded at 340 K immediately after the addition of para-H_2. Spectrum (b) was acquired 80 s later. We didn't observe any enhanced signals, neither from NH/BH intermediates nor from the reaction product 2b. Spectrum (c) recorded after cooling the solution to room temperature approximately two hours after beginning of the reaction showed increased signals of C-H and N-H hydrogens of amine 2b.

5.2 Hydrogenation of alkenes using intermolecular FLPs

Scheme 4. Hydrogenation of 1,1-diphenylethylene using B/P FLPs.

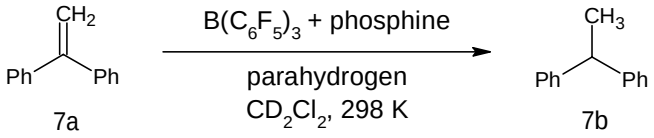

7a 7b

phosphine: P(napht-1-yl)$_3$ (8) $(C_6F_5)PPh_2$ (9)

Scheme 5. Mechanism of alkene hydrogenation via H_2 activation by B/P pair.

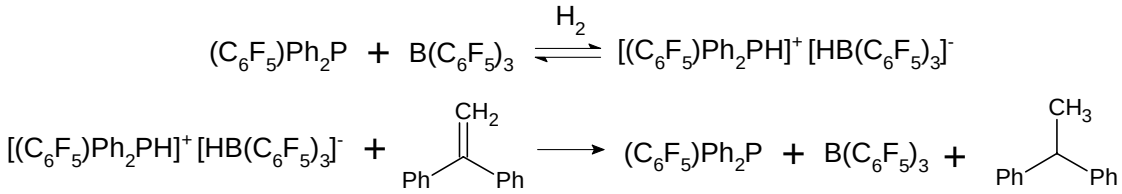

It was reported that alkenes can be hydrogenated with H_2 using B/P FLPs as hydrogen activators.[S7] In this type of reactions B/P pair splits H_2 molecule yielding two intermediates which consequently transfer hydrogens to double bond of alkenes (Scheme 5). Herein, we tested hydrogenations of alkene 7a with para-H_2 using $B(C_6F_5)_3$ (borane 5, see Scheme S2) as Lewis acid and phosphines 8 and 9 (Scheme 4) as Lewis bases.

5.2.1 Hydrogenation of alkene **7a** using P(napht-1-yl)$_3$ (**8**)

In this experiment, we used a solution of 0.1 mmol of 7a, 0.02 mmol of B(C_6F_5)$_3$ and P(napht-1-yl)$_3$ in CD_2Cl_2. Para-H_2 was introduced into the reaction mixture by shaking a sample tube charged with 6 atm of para-H_2.

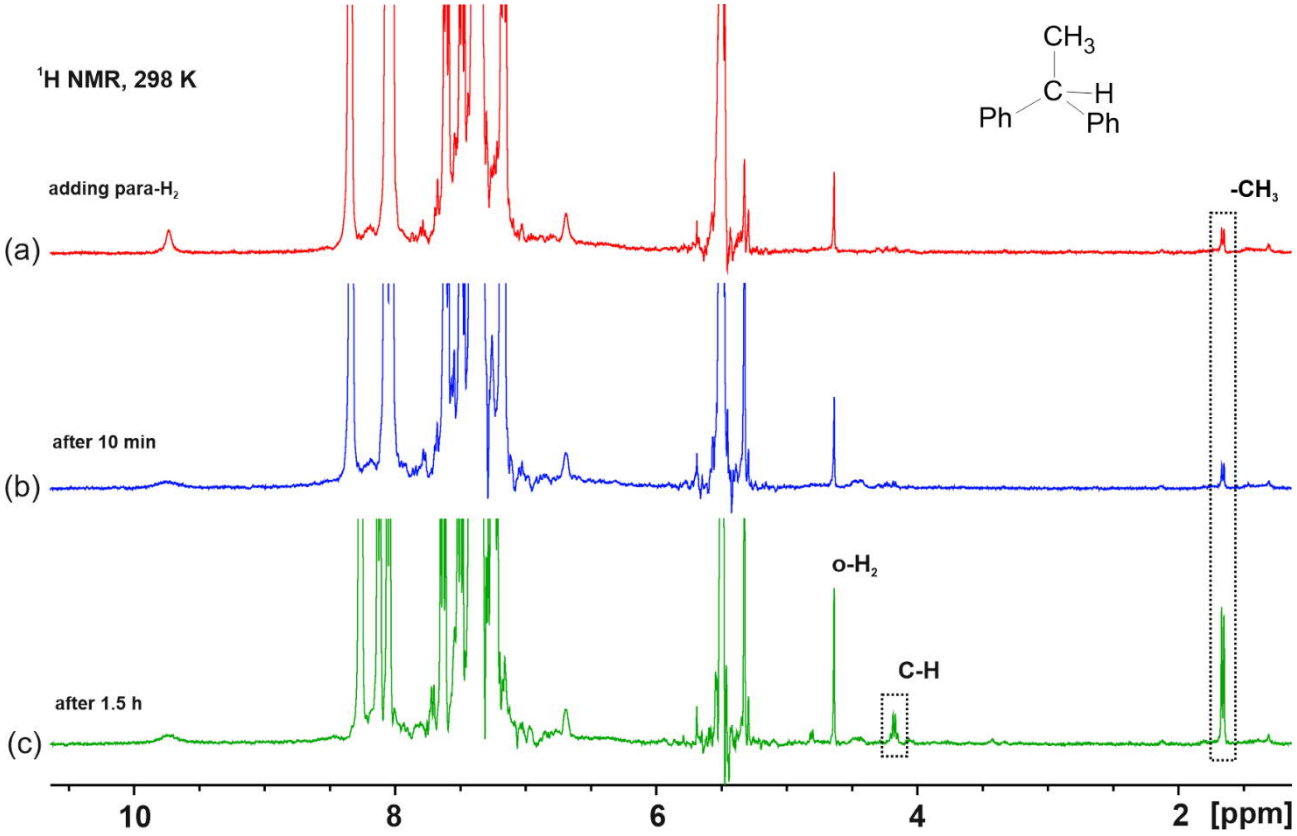

Figure S13. ^{1}H NMR spectra acquired in hydrogenation of alkene 7a with para-H_2 using B(C_6F_5)$_3$ and phosphine 8. Spectrum (a) was recorded at 298 K after the addition of para-H_2. Spectrum (b) was acquired 10 min later. We didn't observe any enhanced signals, neither from PH/BH intermediates nor from the reaction product 7b. Spectrum (c) recorded 1.5 hours after beginning of the reaction showed increased signals of alkane product 7b, indicating the activity of the reaction.

5.2.2 Hydrogenation of alkene **7a** using $(C_6F_5)PPh_2$ (**9**)

In this experiment, we used a solution of 0.1 mmol of 7a, 0.02 mmol of $B(C_6F_5)_3$ and $(C_6F_5)PPh_2$ in CD_2Cl_2. Para-H_2 was introduced into the reaction mixture by shaking a sample tube charged with 6 bar of para-H_2.

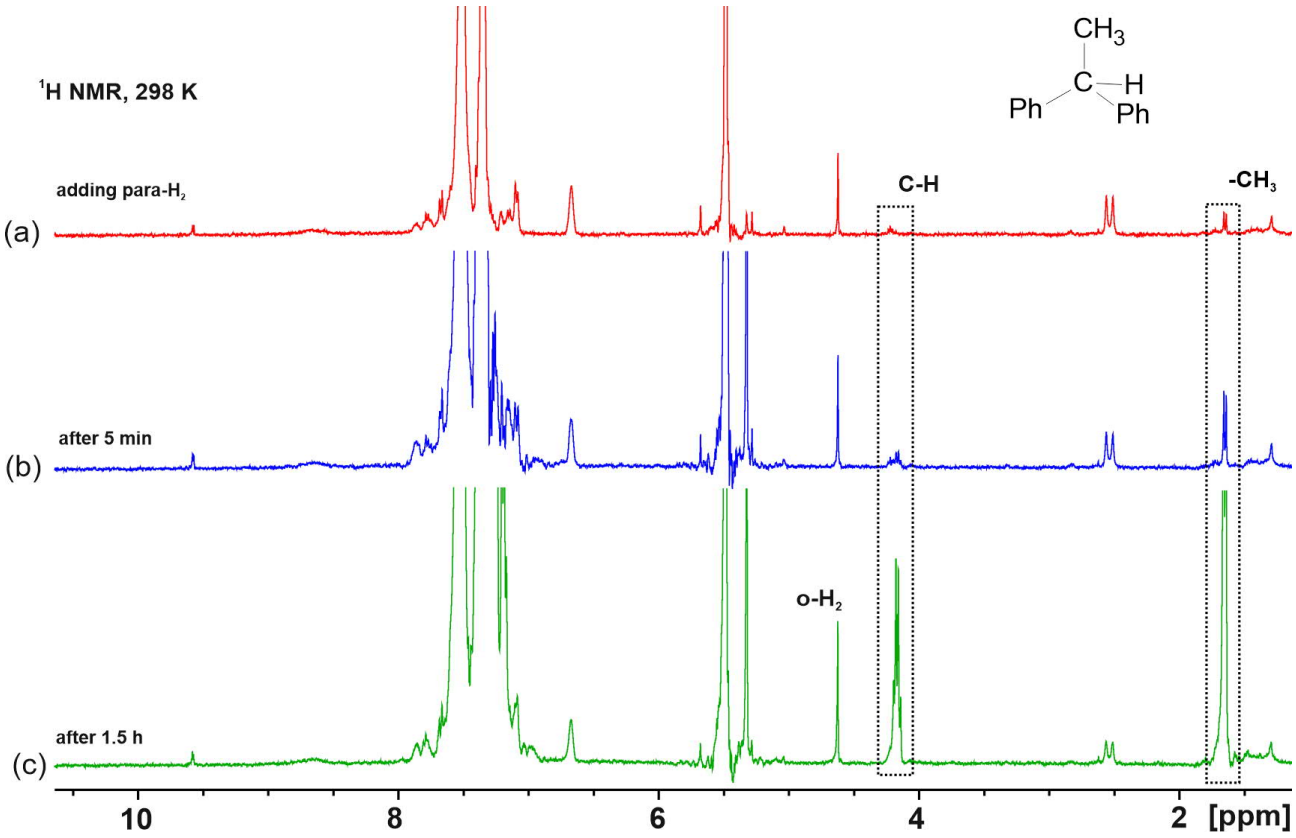

Figure S14. ^{1}H NMR spectra acquired in hydrogenation of alkene 7a with para-H_2 using $B(C_6F_5)_3$ and phosphine 9. Spectrum (a) was recorded at 298 K after addition of para-H_2. Spectrum (b) was acquired 5 min later. We couldn't observe any hyperpolarized signals, neither from PH/BH intermediates nor from the reaction product. Spectrum (c) recorded after 1.5 hours from beginning of the reaction showed increased signals of the alkane product 7b with larger intensities than in the experiment with phosphine 8, showing higher reaction rate with phosphine 9.

6 References

S1. V. Sumerin, K. Chernichenko, M. Nieger, M. Leskel, B. Rieger and T. Repo, Adv. Synth. Catal., 2011, 353, 2093-2110.

S2. D. Chen, Y. Wang and J. Klankermayer, Angew. Chem. Int. Ed., 2010, 49, 9475-9478.

S3. C. R. Bowers and D. P. Weitekamp, J. Am. Chem. Soc., 1987, 109, 5541-5542.

S4. C. R. Bowers, in Encyclopedia of Nuclear Magnetic Resonance, eds. D. M. Grant and R. K. Harris, Wiley, Chichester, 2002, vol. 9, ch. Chapter, pp. 750-769.

S5. D. Chen and J. Klankermayer, Chem. Commun., 2008, 18, 2130-2131

S6. A. Hamza, K. Sorochkina, B. Kótai, K. Chernichenko, D. Berta, M. Bolte, M. Nieger, T. Repo, and I. Pápai, ACS Catal., 2020, 10, 14290-14301.

S7. L. Greb, P. Oña-Burgos, B. Schirmer, S. Grimme, D. W. Stephan and J. Paradies, Angew. Chem. Int. Ed., 2012, 51, 10164-10168.